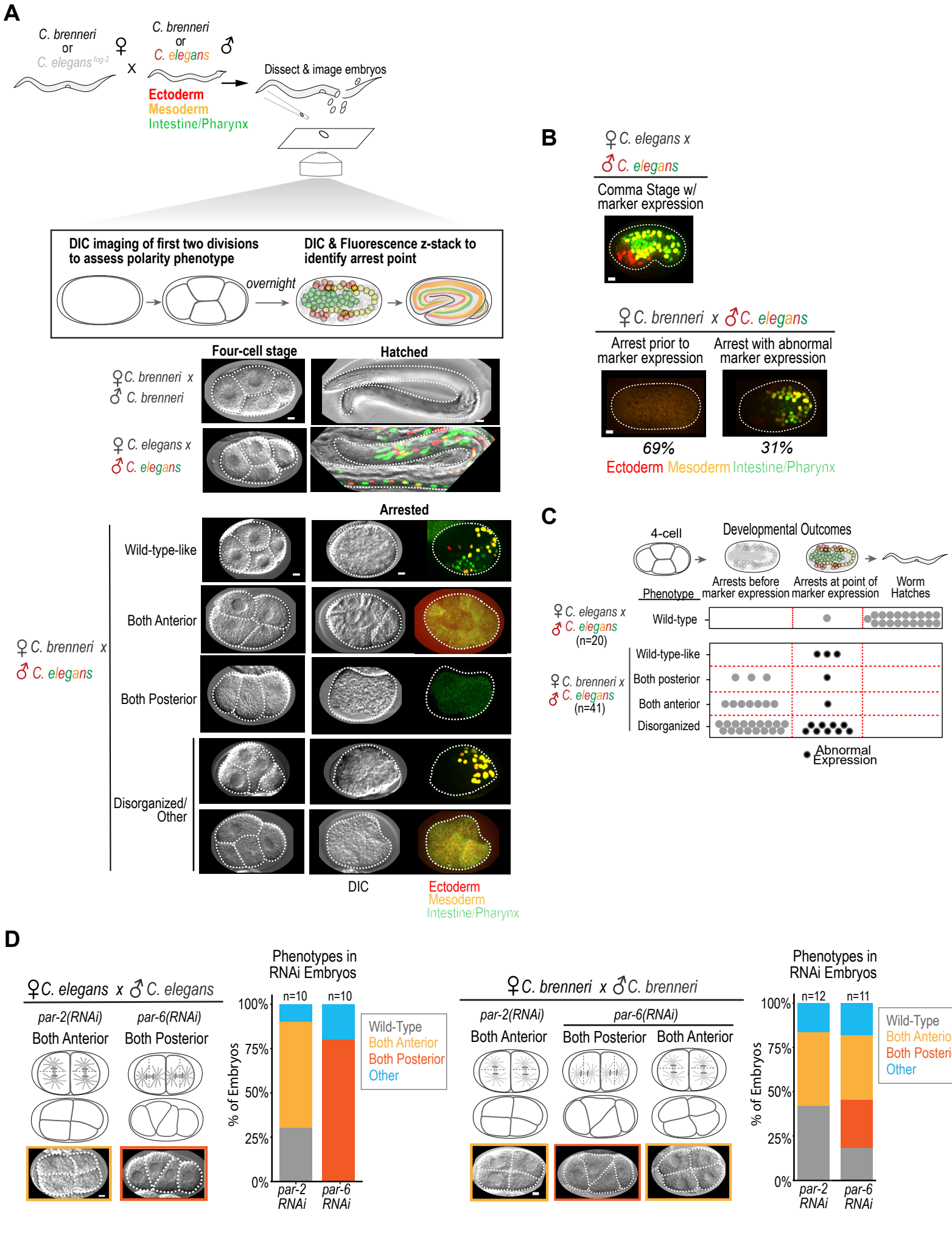
A
C. brenneri or C. elegans fog-2
♀
x
C. brenneri or C. elegans
♂
Ectoderm
Mesoderm
Intestine/Pharynx
Dissect & image embryos
DIC imaging of first two divisions to assess polarity phenotype
DIC & Fluorescence z-stack to identify arrest point
overnight
Four-cell stage
Hatched
♀C. brenneri x ♂C. brenneri
♀C. elegans x ♂C. elegans
Arrested
♀C. brenneri x ♂C. elegans
Wild-type-like
Both Anterior
Both Posterior
Disorganized/ Other
DIC
Ectoderm
Mesoderm
Intestine/Pharynx
B
♀C. elegans x ♂C. elegans
Comma Stage w/ marker expression
♀C. brenneri x ♂C. elegans
Arrest prior to marker expression
Arrest with abnormal marker expression
69%
31%
Ectoderm Mesoderm Intestine/Pharynx
C
4-cell
Developmental Outcomes
Phenotype
Arrests before marker expression
Arrests at point of marker expression
Worm Hatches
♀C. elegans x ♂C. elegans (n=20)
Wild-type
♀C. brenneri x ♂C. elegans (n=41)
Wild-type-like
Both posterior
Both anterior
Disorganized
Abnormal Expression
D
♀C. elegans x ♂C. elegans
par-2(RNAi)
Both Anterior
par-6(RNAi)
Both Posterior
Phenotypes in RNAi Embryos
n=10
n=10
100%
75%
50%
25%
0%
% of Embryos
par-2 RNAi
par-6 RNAi
Wild-Type
Both Anterior
Both Posterior
Other
♀C. brenneri x ♂C. brenneri
par-2(RNAi)
Both Anterior
par-6(RNAi)
Both Posterior
Both Anterior
Phenotypes in RNAi Embryos
n=12
n=11
100%
75%
50%
25%
0%
% of Embryos
par-2 RNAi
par-6 RNAi
Wild-Type
Both Anterior
Both Posterior
Other

Figure S1. Polarity defects at the 4-cell stage correlate with the failure of hybrid embryos to reach mid-embryogenesis and turn on tissue-specific markers, related to Figure 1. (A) The schematic illustrates the experimental workflow to correlate early defects before ZGA, which occurs at the 4-cell stage, with the ability of embryos to reach mid-embryogenesis and turn on tissue-specific markers. Briefly, *C. brenneri* or *C. elegans* females were mated to males from either *a C. elegans* strain in which the genome encodes fluorescent reporters that mark nuclei in the endoderm (*green*), mesoderm (*yellow*), and ectoderm (*red*) or *C. brenneri (unmarked)*. DIC imaging was used to film embryos through the 4-cell stage. A spinning disk confocal fluorescence z-stack was collected of the same embryos 20-24 hours later to identify the point of arrest and determine whether the tissue-specific markers had turned on. Endpoint images for larval worms are scaled to best highlight marker expression, and intensity levels are not directly comparable to the arrested hybrid embryos. **(B)** Representative maximum intensity projections of spinning disc confocal z-stacks of hybrid embryos that arrested prior to (*bottom left*) and after (*bottom right*) the onset of marker expression compared to the comma stage in control *C. elegans* intraspecies embryos (*top*). Image projections are scaled to best highlight marker expression and intensities cannot be directly compared between *C. elegans* and hybrid embryos. (**C**) Summary table displaying the results of the phenotypic analysis for the *C. elegans* and *C. brenneri* x *C. elegans* hybrid embryos. While the majority of *C.* elegans embryos (19/20) showed a wild-type 4-cell phenotype and hatched, most hybrid embryos (38/41) showed a non-wild-type-like 4-cell phenotype, and none hatched. All 3 of the hybrid embryos that exhibited a wild-type-like 4-cell orientation survived to express markers, whereas embryos exhibiting more severe polarity phenotypes rarely made it to marker expression (Both Anterior (1/4); Both Posterior (1/9)). Hybrid embryos that fell into the Disorganized/Other category had an intermediate level of success with 9/26 surviving to the point of marker expression. **(D)** DIC images of representative 4-cell stage embryos are shown for *par-2(RNAi)* and *par-6(RNAi) C. elegans* (*left*) and *C. brenneri* (*right*) embryos. The schematics highlight the 2-cell division planes giving rise to the 4-cell phenotypes, and the graphs show the phenotype frequencies for each condition. Scale bars, 5μm.

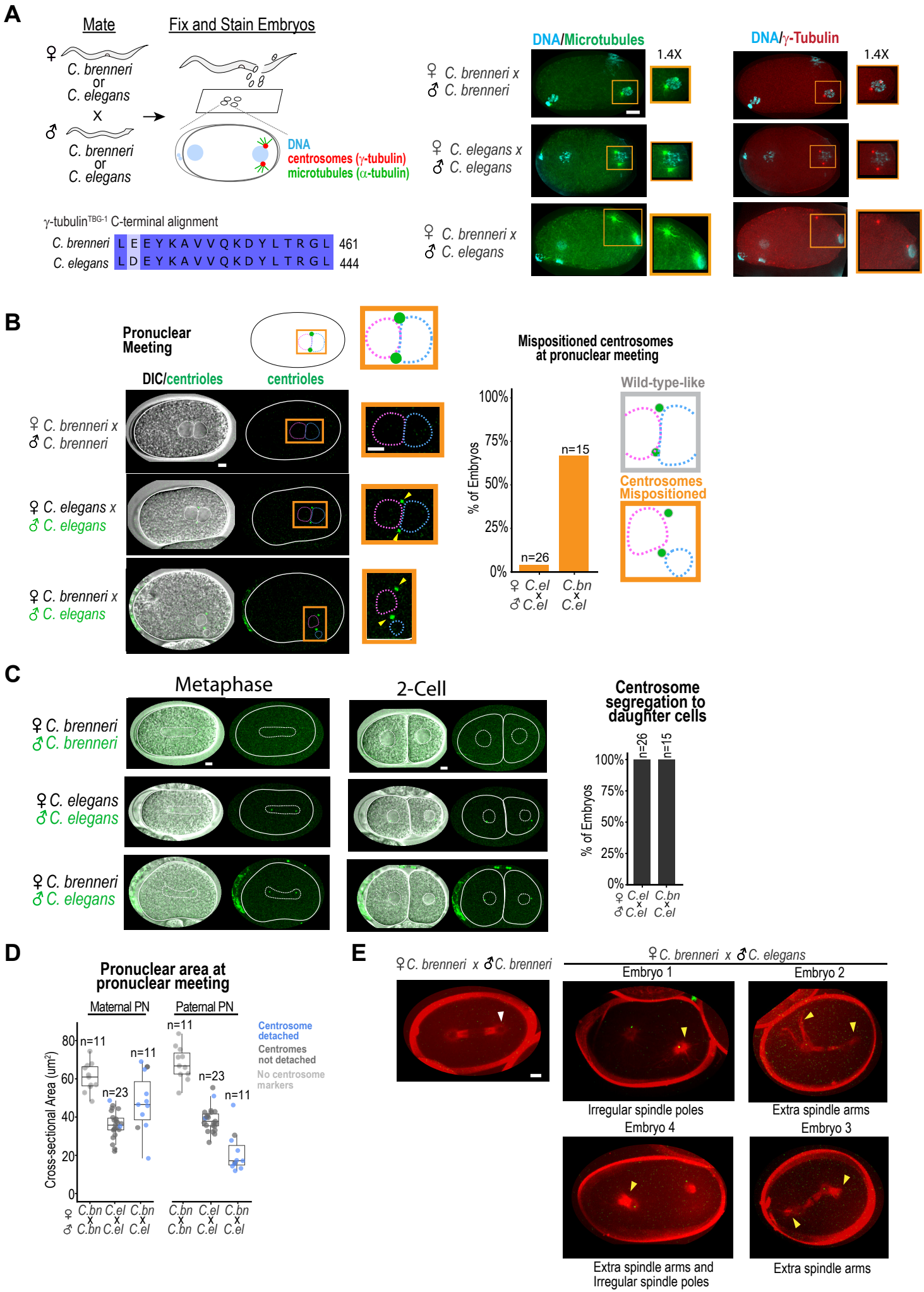
A
Mate
Fix and Stain Embryos
♀ C. brenneri or C. elegans
x
♂ C. brenneri or C. elegans
DNA
centrosomes (γ-tubulin)
microtubules (α-tubulin)
γ-tubulin^TBG-1 C-terminal alignment
C. brenneri L E E Y K A V V Q K D Y L T R G L 461
C. elegans L D E Y K A V V Q K D Y L T R G L 444
DNA/Microtubules
DNA/γ-Tubulin
1.4X
♀ C. brenneri x ♂ C. brenneri
♀ C. elegans x ♂ C. elegans
♀ C. brenneri x ♂ C. elegans
B
Pronuclear Meeting
DIC/centrioles
centrioles
♀ C. brenneri x ♂ C. brenneri
♀ C. elegans x ♂ C. elegans
♀ C. brenneri x ♂ C. elegans
Mispositioned centrosomes at pronuclear meeting
% of Embryos
100%
75%
50%
25%
0%
n=26
n=15
♀ C.el x ♂ C.el
C.bn x C.el
Wild-type-like
Centrosomes Mispositioned
C
Metaphase
2-Cell
♀ C. brenneri ♂ C. brenneri
♀ C. elegans ♂ C. elegans
♀ C. brenneri ♂ C. elegans
Centrosome segregation to daughter cells
% of Embryos
n=26
n=15
♀ C.el x ♂ C.el
C.bn x C.el
D
Pronuclear area at pronuclear meeting
Maternal PN
Paternal PN
Cross-sectional Area (um²)
n=11
n=23
n=11
n=11
n=23
n=11
Centrosome detached
Centromes not detached
No centrosome markers
♀ C.bn x ♂ C.bn
C.el x C.el
C.bn x C.el
E
♀C. brenneri x ♂C. brenneri
♀C. brenneri x ♂C. elegans
Embryo 1
Embryo 2
Irregular spindle poles
Extra spindle arms
Embryo 4
Embryo 3
Extra spindle arms and Irregular spindle poles
Extra spindle arms

Figure S2. Hybrids exhibit defects in centrosome-pronuclear attachment and spindle morphology, related to Figures 2 and 3. (A) (*left*) The schematic illustrates the mating regime and the predicted staining patterns of α-tubulin, the centrosomal marker γ-tubulin, and DNA. An alignment of the C-terminal peptide of *C. elegans* γ-tubulin (TBG-1), against which the antibody was raised, to the equivalent region of the *C. brenneri* protein. (*right*) Representative images of 1-cell stage *C. brenneri* (n = 14), *C. elegans* (n = 12), and hybrid (n = 12) embryos after the conversion of centrioles to centrosomes but prior to pronuclear migration stained for DNA (*cyan*), α-tubulin (DM1α) (*green*), and γ-tubulin (*red*). Insets are magnified 1.4X. One or both centrosomes were usually detached in hybrids (11/12 embryos). Maximum intensity projections were scaled to best highlight protein localization, so intensity levels are not directly comparable across images. (**B**) (*left*) Paired DIC/fluorescence overlay and fluorescence-only images of *C. brenneri*, *C. elegans,* and hybrid pronuclear meeting stage 1-cell embryos. The schematic on top illustrates the expected position of the mCherry::SAS-4 marked centrioles (*green*). White solid lines trace the embryo. Dashed lines trace pronuclei; in fluorescence images, the sperm and oocyte-derived pronuclei are traced in blue and magenta, respectively. Insets are magnified 2.3X. Yellow arrowheads mark centrosomes. Image intensities are scaled to highlight centriole localization and cannot be compared across images. (*right*) The graph quantifies the percentage of embryos with wild-type-like (*gray box*) and mispositioned (*orange box*) centrosomes at pronuclear meeting. **(C)** Paired DIC/fluorescence overlay (*left*) and fluorescence-only (*right*) images of *C. brenneri*, *C. elegans,* and hybrid embryos at metaphase of the first division and the 2-cell stage. White solid lines outline the embryos and white dotted lines outline the spindle (metaphase) or nuclei (2-cell). Images are different timepoints taken from timelapse series of the same embryos shown in *Figure 2D*, *Figure S2B*. Image intensities for centrioles were scaled to best show centrosome localization and cannot be directly compared across embryos. The graph plots the percent of embryos that show the correct segregation of one sperm-derived centriole into each daughter cell (26/26 embryos in *C. elegans*; 15/15 embryos in hybrids). (**D**) *C. brenneri* females were mated with *C. brenneri* males as a control or with *C. elegans* males with mCherry::SAS-4-marked centrioles (*green*) and were dissected into the vital dye SiR-tubulin (*red*) to monitor microtubules as described in *Figure 3D*. Images are maximum intensity projections that capture SiR-tubulin-stained spindles (*red*) in a *C. brenneri* embryo (*top, left)* and four examples of hybrid embryos at anaphase. The white arrowhead indicates normal spindle morphology, whereas yellow arrowheads point to spindle poles or extra spindle arms in hybrid embryos. Embryos categorized as having abnormal spindles in the graph in *Figure 3D* displayed phenotypes similar to the ones shown here. Intensities were scaled to best show SiR-tubulin signal and cannot be compared across embryos. Centriole intensities are scaled the same across images. *C. brenneri* embryos do not contain marked centrioles. Scale bars, 5μm.

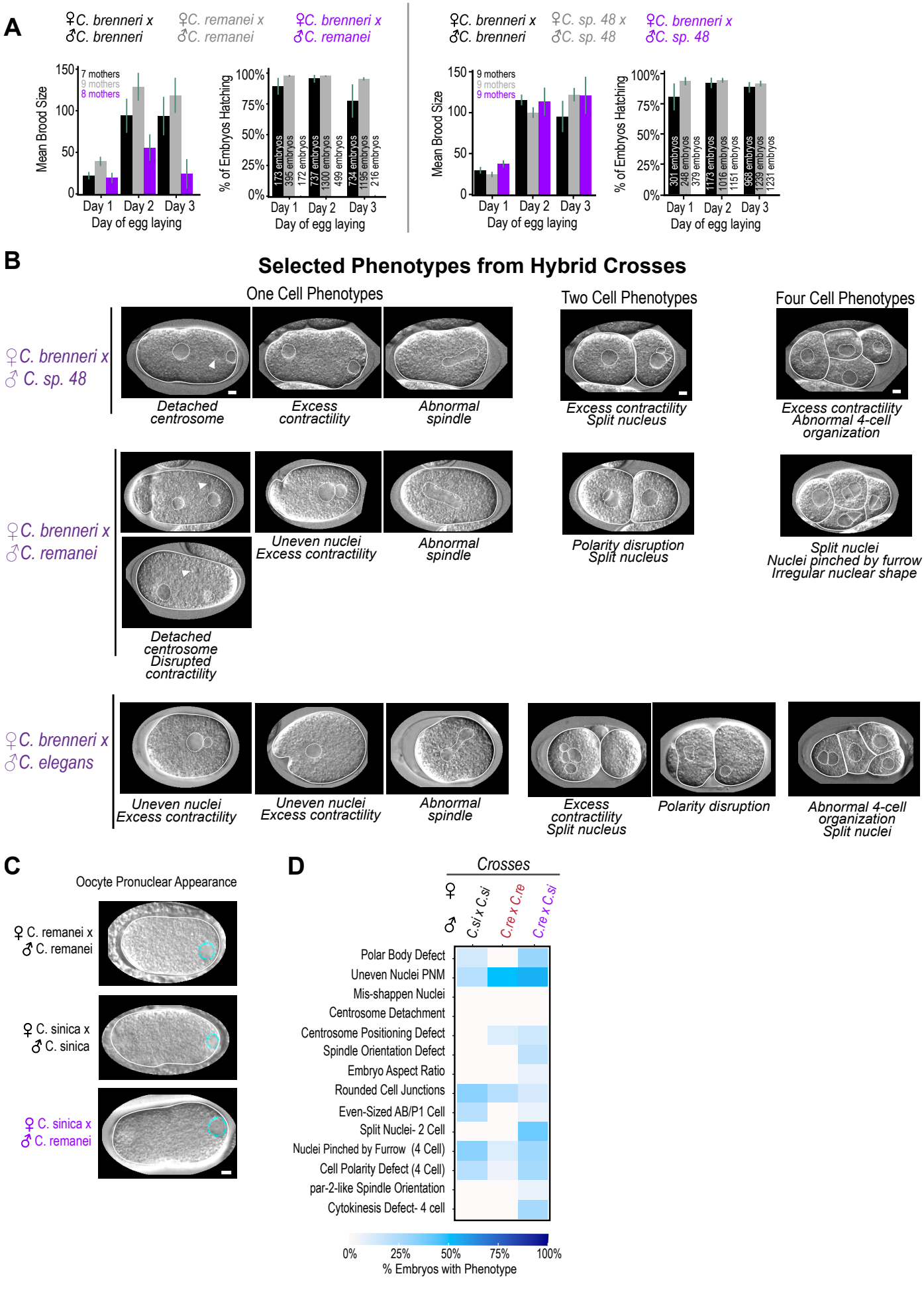
A
♀C. brenneri x ♂C. brenneri
♀C. remanei x ♂C. remanei
♀C. brenneri x ♂C. remanei
Mean Brood Size
7 mothers
9 mothers
8 mothers
Day 1 Day 2 Day 3
Day of egg laying
% of Embryos Hatching
173 embryos 395 embryos 172 embryos
737 embryos 1300 embryos 499 embryos
734 embryos 1195 embryos 216 embryos
♀C. brenneri x ♂C. brenneri
♀C. sp. 48 x ♂C. sp. 48
♀C. brenneri x ♂C. sp. 48
9 mothers
9 mothers
9 mothers
301 embryos 248 embryos 379 embryos
1173 embryos 1016 embryos 1151 embryos
968 embryos 1239 embryos 1231 embryos
B
Selected Phenotypes from Hybrid Crosses
One Cell Phenotypes
Two Cell Phenotypes
Four Cell Phenotypes
♀C. brenneri x ♂ C. sp. 48
Detached centrosome
Excess contractility
Abnormal spindle
Excess contractility Split nucleus
Excess contractility Abnormal 4-cell organization
♀C. brenneri x ♂C. remanei
Uneven nuclei Excess contractility
Abnormal spindle
Polarity disruption Split nucleus
Split nuclei Nuclei pinched by furrow Irregular nuclear shape
Detached centrosome Disrupted contractility
♀C. brenneri x ♂C. elegans
Uneven nuclei Excess contractility
Uneven nuclei Excess contractility
Abnormal spindle
Excess contractility Split nucleus
Polarity disruption
Abnormal 4-cell organization Split nuclei
C
Oocyte Pronuclear Appearance
♀ C. remanei x ♂ C. remanei
♀ C. sinica x ♂ C. sinica
♀ C. sinica x ♂ C. remanei
D
Crosses
♀ ♂
C.si x C.si
C.re x C.re
C.re x C.si
Polar Body Defect
Uneven Nuclei PNM
Mis-shappen Nuclei
Centrosome Detachment
Centrosome Positioning Defect
Spindle Orientation Defect
Embryo Aspect Ratio
Rounded Cell Junctions
Even-Sized AB/P1 Cell
Split Nuclei- 2 Cell
Nuclei Pinched by Furrow (4 Cell)
Cell Polarity Defect (4 Cell)
par-2-like Spindle Orientation
Cytokinesis Defect- 4 cell
0% 25% 50% 75% 100%
% Embryos with Phenotype

Figure S3. Gallery of hybrid phenotypes, related to Figure 4. (**A**) Graphs show the average brood size and % hatching for the embryos collected during the indicated days for the indicated species (*grey*, *black*) or hybrid (*purple*) cross. Day 1 is 0-24 hours post-mating; day 2 is 24-44 hours post-mating; day 3 is 44-64 hours post-mating. n refers to the number of embryos counted per cross. Error bars are ± SE. (**B**) The gallery highlights abnormal phenotypes found in 1, 2, and 4-cell hybrid embryos from *C. brenneri* females crossed with males from *C. sp. 48* (*top*), *C. remanei* (*middle*), and *C. elegans* (*fog-2(q71)*; *bottom*). White solid lines outline the embryos and white dotted lines outline the pronuclei, spindle, and nuclei. Yellow arrowheads highlight detached centrosomes. (**C**) DIC images of embryos at the oocyte pronuclear appearance stage for the indicated crosses. Solid white lines trace the perimeter of the embryos and dashed cyan dashed lines trace the perimeter of the sperm-derived pronuclei. (**D**) The heatmap summarizes embryonic defects observed through the 4-cell stage for the indicated crosses; embryos were scored blinded to cross. Shading from white to dark blue indicates phenotype penetrance. Scale bars, 5μm.

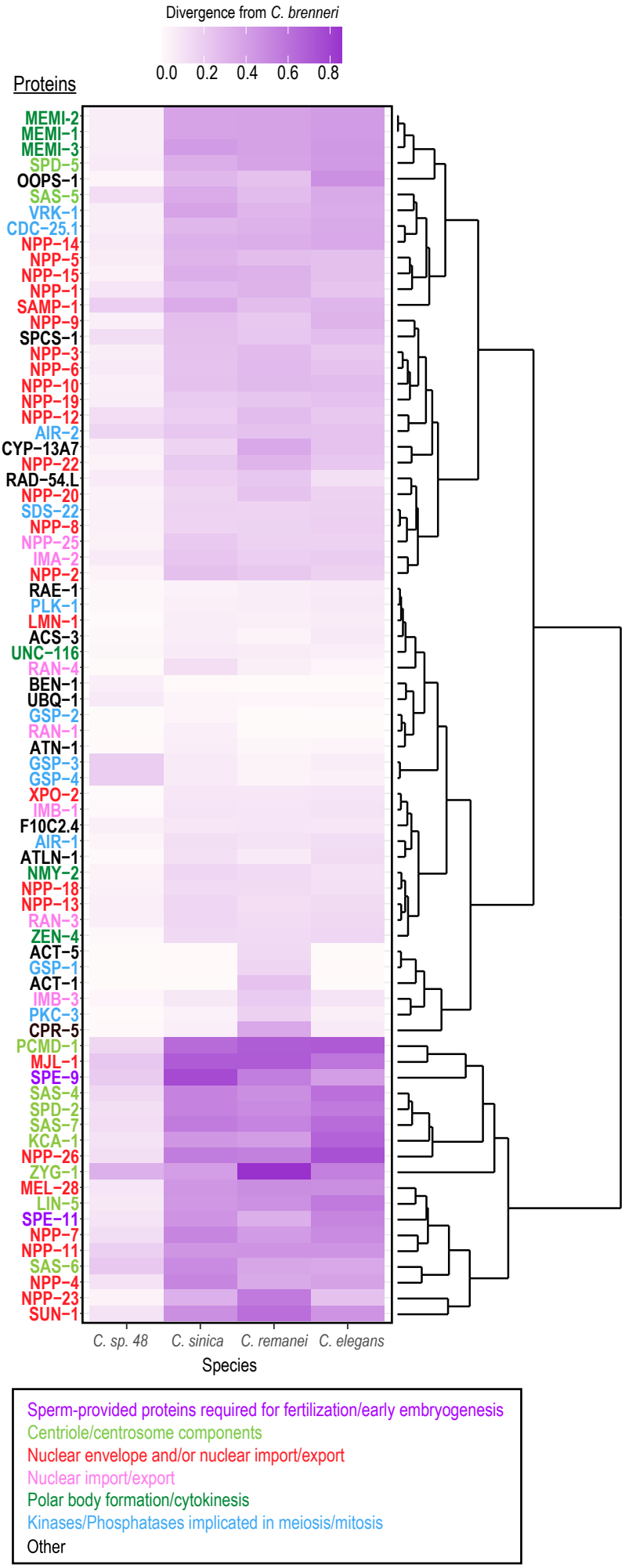
Divergence from C. brenneri
0.0 0.2 0.4 0.6 0.8
Proteins
MEMI-2
MEMI-1
MEMI-3
SPD-5
OOPS-1
SAS-5
VRK-1
CDC-25.1
NPP-14
NPP-5
NPP-15
NPP-1
SAMP-1
NPP-9
SPCS-1
NPP-3
NPP-6
NPP-10
NPP-19
NPP-12
AIR-2
CYP-13A7
NPP-22
RAD-54.L
NPP-20
SDS-22
NPP-8
NPP-25
IMA-2
NPP-2
RAE-1
PLK-1
LMN-1
ACS-3
UNC-116
RAN-4
BEN-1
UBQ-1
GSP-2
RAN-1
ATN-1
GSP-3
GSP-4
XPO-2
IMB-1
F10C2.4
AIR-1
ATLN-1
NMY-2
NPP-18
NPP-13
RAN-3
ZEN-4
ACT-5
GSP-1
ACT-1
IMB-3
PKC-3
CPR-5
PCMD-1
MJL-1
SPE-9
SAS-4
SPD-2
SAS-7
KCA-1
NPP-26
ZYG-1
MEL-28
LIN-5
SPE-11
NPP-7
NPP-11
SAS-6
NPP-4
NPP-23
SUN-1
C. sp. 48
C. sinica
C. remanei
C. elegans
Species
Sperm-provided proteins required for fertilization/early embryogenesis
Centriole/centrosome components
Nuclear envelope and/or nuclear import/export
Nuclear import/export
Polar body formation/cytokinesis
Kinases/Phosphatases implicated in meiosis/mitosis
Other

Figure S4. Sequence divergence in early embryonic proteins, related to Figure 4. (**A**) Heat map of protein sequence divergence scores of early embryonic proteins between *C. brenneri* and *C. sp. 48*, *C. sinica*, *C. remanei*, and *C. elegans*. Scores represent level of divergence from *C. brenneri* protein sequences, while the phylogeny clusters protein divergence scores based on similarity across all species compared to *C. brenneri*. The level of divergence is 1 – BLOSUM62 score (Biopython[S1]). Gene names are color-coded as indicated in the key below the heat map. Proteins encoded by genes in the Phenobank phenotypic classes pronuclear appearance, asymmetry of division, centrosome attachment, and spindle assembly were subjected to pairwise protein sequence divergence analysis. To compare protein sequence divergence between *C. brenneri* and the species crossed with it in this study, as well *C. sinica*, we pulled out and clustered *C. brenneri* protein pairwise divergence scores versus all other species. Protein sequences clustered in 4 groups, with low divergence genes clustering with conserved genes like UBQ-1,[S2] and high divergence genes clustering with sperm genes like SPE-9 and SPE-11. Interestingly, a number of proteins involved in the formation and structure of nuclear pore complexes, such as MEL-28, NPP-7, NPP-4, NPP-23, and NPP-11[S3-9] clustered with high divergence genes. We note that SPE-11, a sperm-provided protein implicated in polar body formation[S10,S11] and KCA-1, a kinesin-1 binding protein implicated in maintaining sperm centrioles in a quiescent state until after the second polar body is extruded during anaphase of meiosis II,[S12] also exhibit high divergence. While this protein sequence divergence analysis is biased towards genes associated with phenotypes we see in hybrids, it represents a starting point to identify proteins that may play a functional role in hybrid incompatibility between *C. brenneri* females and males of other species in the *Elegans* group.

SUPPLEMENTAL REFERENCES LIST

S1. Cock, P. J. *et al.* (2009). Biopython: freely available Python tools for computational molecular biology and bioinformatics. *Bioinformatics* **25**, 1422.

S2. Kasimatis, K. R. & Phillips, P. C. (2018). Rapid Gene Family Evolution of a Nematode Sperm Protein Despite Sequence Hyper-conservation. *G3 Genes*|*Genomes*|*Genetics* **8**, 353–362.

S3. Galy, V., Askjaer, P., Franz, C., López-Iglesias, C. & Mattaj, I. W. (2006). MEL-28, a Novel Nuclear-Envelope and Kinetochore Protein Essential for Zygotic Nuclear-Envelope Assembly in C. elegans. *Current Biology* **16**, 1748–1756.

S4. Gómez-Saldivar, G. *et al.* (2016). Identification of Conserved MEL-28/ELYS Domains with Essential Roles in Nuclear Assembly and Chromosome Segregation. *PLOS Genetics*.

S5. Askjaer, P. Modern Tools to Study Nuclear Pore Complexes and Nucleocytoplasmic Transport in Caenorhabditis elegans.

S6. Martino, L., Joly, N. & Desai, A. Channel Nucleoporins Recruit PLK-1 to Nuclear Pore Complexes to Direct Nuclear Envelope Breakdown in C. elegans.

S7. Voronina, E. & Seydoux, G. The C. elegans homolog of nucleoporin Nup98 is required for the integrity and function of germline P granules.

S8. Walther, T. C., Fornerod, M., Pickersgill, H., Goldberg, M., Allen, T. D. & Mattaj, I. W. (2001). The nucleoporin Nup153 is required for nuclear pore basket formation, nuclear pore complex anchoring and import of a subset of nuclear proteins. *The EMBO journal*.

S9. Ródenas, E., González-Aguilera, C., Ayuso, C. & Askjaer, P. (2012). Dissection of the NUP107 nuclear pore subcomplex reveals a novel interaction with spindle assembly checkpoint protein MAD1 in *Caenorhabditis elegans*. *MBoC* **23**, 930–944.

S10. McNally, K. L. & McNally, F. J. (2005). Fertilization initiates the transition from anaphase I to metaphase II during female meiosis in C. elegans. *Developmental Biology* **282**, 218–230.

S11. Hill, D. P., Shakes, C., Ward, S. & Strome, S. (1989). A Sperm-Supplied Product Essential

for Initiation of Normal Embryogenesis in Caenorhabditis elegans Is Encoded by the Paternal-Effect Embryonic-Lethal Gene, spe-7 l. doi:10.1016/0012-1606(89)90138-3.

S12. McNally, K. L. P., Fabritius, A. S., Ellefson, M. L., Flynn, J. R., Milan, J. A. & McNally, F. J. (2012). Kinesin-1 Prevents Capture of the Oocyte Meiotic Spindle by the Sperm Aster. *Developmental Cell* **22**, 788–798.